Arabian Journal of Chemistry (2022) **15**, 104233

King Saud University

Arabian Journal of Chemistry

www.ksu.edu.sa
www.sciencedirect.com

ORIGINAL ARTICLE

Improving hydrophobicity and compatibility between kenaf fiber and polymer composite by surface treatment with inorganic nanoparticles

Mohammed Mohammed [a,b,*], Rozyanty Rahman [a,b,*], Aeshah M. Mohammed [c], Bashir O. Betar [e], Azlin F. Osman [a,b], Tijjani Adam [d], Omar S. Dahham [f,g], Subash C.B. Gopinath [b,h]

[a] *Center of Excellence Geopolymer & Green Technology (CEGeoGTech), Universiti Malaysia Perlis, 02600 Arau, Perlis, Malaysia*
[b] *Faculty of Chemical Engineering Technology, Universiti Malaysia Perlis (UniMAP), Arau 02600, Perlis, Malaysia*
[c] *University of Bagdad College of Education for Pure Science Ibn-Alhaitham, Iraq*
[d] *Faculty of Electronics Engineering Technology, Universiti Malaysia Perlis, Kampus Uniciti Alam Sg. Chuchuh, 02100 Padang Besar (U), Perlis, Malaysia*
[e] *Research Center (NANOCAT), University of Malaya, Kuala Lumpur 50603, Malaysia*
[f] *Department of Civil Engineering, College of Engineering, Cihan University-Erbil, Kurdistan Region, Iraq*
[g] *Department of Petroleum and Gas Refinery Engineering, Al-Farabi University College, Baghdad, Iraq*
[h] *Institute of Nano Electronic Engineering, Universiti Malaysia Perlis, Perlis, Malaysia*

Received 8 September 2021; accepted 31 August 2022
Available online 7 September 2022

KEYWORDS

Natural fiber;
Nanocomposites;
Surface treatment;
Nano zinc oxide

Abstract Compatibility of natural fiber with hydrophobic matrix is a herculean task in literature works. Surface treatment is a well-known approach for increasing the strength of interfacial adhesion between fibres and polymer matrices. Therefore, this study aims to examine the impact of surface treatment with zinc oxide nanoparticles (ZnONPs) in improving hydrophobicity of kenaf fiber (KF) to enhance the compatibility between KF and polymer matrix. In this study, KF reinforced unsaturated polyester composites (KF/UPE) were fabricated by the hand lay-up method with varying fiber loadings (wt %) of 10 20, 30, and 40. KF were treated with five different contents of ZnONPs (1% to 5 wt%) to make UPE/KF-ZnONPs composites. The composites were studied in terms of wetting response (contact angle measure and water absorption), mechanical properties, chemical structure (FTIR), crystalline structure (XRD), and surface morphology (SEM, AFM).

* Corresponding authors at: Center of Excellence Geopolymer & Green Technology (CEGeoGTech), Universiti Malaysia Perlis, 02600 Arau, Perlis, Malaysia.
E-mail addresses: hmn7575@yahoo.com (M. Mohammed), rozyanty@unimap.edu.my (R. Rahman).
Peer review under responsibility of King Saud University.

Production and hosting by Elsevier

https://doi.org/10.1016/j.arabjc.2022.104233

The investigational findings indicate that the composite samples incorporating ZnONPs exhibit optimum hydrophobicity and mechanical properties, as they possessed a higher contact angle than the untreated KF composite. The optimum content of ZnONPs was found to be 2 wt%. Regarding water absorption, the untreated UPE/KF composites absorbed more water than the treated UPE/KF-ZnONPs composites. SEM images showed changes in the morphology of the KF, while FTIR analysis proved the presence of ZnONPs functional groups in the UPE/KF composites. AFM images revealed that the ZnONPs could actively produce nanolevel roughness, advantageous to the hydrophobic characteristics.

1. Introduction

In comparison to synthetic fibers, natural fibers have been used as potential reinforcement in composite manufacturing sectors to effectively decrease carbon dioxide emissions in the environment and create lighter weight automotive, maritime, and aircraft parts, as well as used as a construction material for structural and non-structural components (Sanjay et al., 2018; Dicker et al., 2014). These fibers have several benefits, namely high specific strength, relatively inexpensive, lightweight, renewability, biodegradability, lack of related health concerns, simplicity of surface modification, widespread availability, and relatively low abrasiveness (Jumaidin et al., 2016; Baghaei et al., 2014). Additionally, natural fibers have demonstrated superior features such as minimum tool wear, good thermal conductivity, low energy consumption, and adequate tensile strength compared to synthetic fibers (Karthikeyan et al., 2017). Natural fiber composites also have superior mechanical characteristics to glass fiber composites (Sezgin and Berkalp, 2017). All-natural fibers are comprised of cellulose, hemicellulose, lignin, and pectin. Furthermore, natural fibers such as kenaf, hemp, and jute are primarily composed of cellulose and lignin (Dittenber and GangaRao, 2012). Cellulose is a semi-crystalline polysaccharide hydrophilic component comprised of a linear chain of anhydrous glucose units containing alcoholic hydroxyl groups. As a result, all-natural fibers are hydrophilic (Mohanty et al., 2005).

On the other hand, natural fibers have several drawbacks, including low transverse and compressive strengths and significant temperature and moisture sensitivity (Belaadi et al., 2014). The effectiveness of fiber-reinforced composites is determined by the fiber–matrix interface and the capacity of the matrix to transfer stress to the fiber (Valadez-Gonzalez et al., 1999). The experimental work done by Kumar and Sekaran (Kumar and Sekaran, 2014) indicated that the primary impediments to using natural fibers in plastics had been their low compatibility with the matrix and their inherent high moisture absorption, which can contribute to dimensional changes in the fibers, as well as propagation cracks in the composite and deterioration of mechanical properties. The surface of the natural fiber has polar hydroxyl groups; these hydroxyl groups have trouble forming well-bonded interphase with the relatively nonpolar polymer matrix (Akil et al., 2011). Additionally, it was shown by Wambua et al. that the integration of nanoparticles into the polymer matrix is frequently associated with agglomeration, mainly due to insufficient dispersion induced by the bias of fiber to form hydrogen bonds with one another (Wambua et al., 2003). A critical property of plant fibers is their capacity to absorb significant amounts of moisture from the environment because of the hygroscopic nature of cellulose. This absorption results in weight and dimension changes and also changes in strength (Mohammed et al., 2017).

One of the critical concerns with natural fibers is the hydrophilicity of cellulose characteristics, which affects the weak interface bonding with hydrophobic polymers used as a matrix. One of the ways to overcome this primary impediment is to chemically modify the fibers to improve the fiber–matrix interface, which includes alkali treatment and coupling agents (Ray et al., 2001, Li et al., 2007; Sreekala and Thomas, 2003). Alkaline treatment is frequently used to remove open hydroxyl groups that tend to interact with water molecules. However, this method exhibited certain drawbacks due to the reduced overall strength characteristics of the fibers and did not significantly enhance interfacial adhesion between fiber and polymer matrix (Dittenber and GangaRao, 2012; Wong et al., 2010). Another frequent method of modifying natural fibers is by the use of a coupling agent. The coupling agent acts in two ways: reacting with the hydroxyl (OH) groups in the cellulose and reacting with the functional groups of matrices to promote stress transfer from the matrix to the fiber (Rozman et al., 2005; Bessadok et al., 2009). However, the efficacy of such modification is highly dependent on the treatment circumstances, such as concentration and duration of treatment, which limit its utilization as a suitable modification of natural fibers (John and Anandjiwala, 2008).

Another way to overcome the hydrophilic and poor performance of natural fiber reinforced polymer composite is by employing nanoparticles in surface treatment. Soltani et al. (Soltani et al., 2013) have measured the impact of zinc oxide nanoparticles (ZnONPs) on the water repellence and dimensional beech wood stability. The results show that the ZnONPs used to adjust wood significantly enhances dimensional stability and decrease wood hygroscopicity. Furthermore, Wang et al. (Wang et al., 2012) have impregnated TiO_2 in Wood composite; as a result of this inorganic modification, the hygroscopicity of wood was considerably decreased, and its dimensional stability was enhanced consequently. An efficient way of evaluating the influence of nano-$CaCO_3$ on the structure and characteristics of holocellulose fiber/polypropylene biomass composites was performed by Li et al. (2017). The results demonstrated that the nano-$CaCO_3$ had a notable impact on the structure and characteristics of the composites. Wang et al. reported that by incorporating inorganic components into the natural fibers and their polymer matrix composites, the natural fibers could be functionalized with improved characteristics in terms of water repellence and resistance to biodegradation (Wang et al., 2012). Wegner et al. also stated that the favourable properties of these modified materials, including absorbing the broadband UV, bio-degradability resistance, eco-friendly characteristics, and resistance to high temperature, provide a way for natural fiber lignocellulosic materials to enhance their efficiency and function (Wegner et al., 2005). A similar study conducted by Freeman and McIntyre (Freeman and McIntyre, 2008) showed that nano-metal particles are available having sizes smaller than the natural fiber pore diameters, resulting in increased penetration and stability. Table 1 lists the published research on the impact of the incorporation of nanoparticles into natural fibers.

Although numerous studies have been reported the impact of surface treatment on natural fibers in terms of water absorption, mechanical performance, and morphology, there is still a scarcity of data. Therefore, the purpose of this study is to assess the effect of surface treatment with zinc oxide nanoparticles (ZnONPs) on enhancing the hydrophobicity of kenaf fibre (KF) in order to improve the compatibility of KF and polymer matrix. This study has been conducted to be the first to demonstrate that surface treatment with nanoparticles is a crucial initial step in providing immunity to natural fiber polymer composites toward quick and unnecessary degradation by promoting

Table 1 The impacts of the incorporation of nanoparticles into natural fibers.

Natural fiber/Nano particles	Achievement	References
Kenaf fiber/nano-SiO_2	The tensile strength, compressive strength, and impact strength increased by 20.61%, 23.71%, and 22.88%, respectively with 2% fraction of nanofiller in composite.	(Jotiram et al., 2022)
Thespesia fiber/ silver nanoparticles (AgNPs)	The thermal stability of the modified fibers was higher than that of the unmodified fibers. The modified fibers exhibited good antibacterial activity against both the Gram negative and Gram-positive bacteria.	(Ashok et al., 2018)
Jute fibre/carbon nano tube	With a 6% fraction of nanofiller in composite, the tensile strength, flexural strength, and impact strength improved, correspondingly.	(Saiteja et al., 2020)
Tamarind fruit shells/copper nanoparticle	The thermal stability of the modified fiber was found to be slightly lower than that of unmodified. The modified fiber exhibited excellent antibacterial activity against both Gram negative and Gram positive bacteria.	(Ashok et al., 2020)
Waste leather trimming/ silver nanoparticles (AgNPs)	The modified Waste leather trimming formed the inhibition zones against E.coli, P. aeruinosa, S.aeureus and B.lichinomonas bacteria	(Ashok et al., 2021)
Basalt fibre / Silicon carbide nano (SiC)	With a 4% nanofiller percentage in composite, the mechanical properties improved. enhanced fibre mat-matrix interfacial interaction Moreover, the composites have superior wear resistance, and had a low capacity for water absorption with 2% wt	(Thooyavan et al., 2022)
Tamarind fruit shell powder/ silver nanoparticles (AgNPs)	The Tamarind fruit shell with in situ generated AgNPs inhibited the growth of bacteria and hence can be used as antibacterial low-cost filler in making biocomposites.	(Li et al., 2019)
Tamarind indica nut power/copper nanoparticle	It was found that these hybrid nanocomposites exhibit excellent antibacterial activity, thermal resistance, and crystallinity. Thus, these bio-based materials can be utilised to replace conventional packaging materials in food packaging, thereby reducing the environmental impact of conventional plastics.	(Kumar et al., 2021)
Tamarind nut powder/copper nanoparticle	The modified Tamarind nut powder displayed significant antibacterial activity against both Gram-negative and Gram-positive bacteria; therefore, it can be utilised as a low-cost filler in the preparation of antibacterial hybrid polymer nanocomposites for packaging and medicinal applications.	(Ashok et al., 2019)
Flax fibre/Titanium dioxide (TiO_2)	When the concentration of TiO_2 in composites was increased from 4% to 6%, the composite's tensile strength climbed to 12.31% and its young's modulus increased to 23.17%.	(Prasad et al., 2018)

water repellency and improving the mechanical characteristics, resulting in the production of natural fiber polymer composites with high water repellency and strength properties. In the published literature, we found no research has been performed to observe the effect of surface treatment with ZnONPs on the hydrophobicity of KF and relate that with improving the mechanical and physical characteristics of its composite. For this aim, we compared treated KF-ZnONPs composites to untreated KF composites using UPE as the matrix in terms of water absorption, mechanical characteristics, SEM micrographs, and FTIR spectrum. The findings will serve as a scientific standard to produce high-performance polymer composites containing KF as reinforcement, particularly in construction purposes such as floor decking, door, and window frames.

2. Materials and experimental methods

2.1. Materials

The National Kenaf and Tobacco Board (NKTB), Kota Bahru, Kelantan, Malaysia, provided the KF in the form of a mat. The unsaturated polyester Reversol P-9565 (UP) resin was utilized as the polymer matrix for the composites during the entire study. Synthomer PLC manufactured the resin, and Dr. Rahmatullah Sdn. Bhd., Bukit Mertajam, Malaysia supplied it. Methyl ethyl ketone peroxide (MEKP) was marketed under the trade name Butanox M-50 by Kaumjung Akzo Nobel and distributed by Hasrat Sdn. Bhd. Butterworth, Malaysia. Sigma-Aldrich (M) Sdn. Bhd. (Kuala Lumpur, Malaysia) provided rod-shaped zinc oxide nanoparticles (ZnONPs).

2.2. Treatment with Nano-ZnO

In this study, the kenaf mat was cut into 20 × 20 × 0.3 cm to length and width, respectively, to be used for further treatment. Surface treatment of KF by using ZnONPs, different percentages of the ZnONPs suspension in distilled water were used, namely 0, 1, 2, 3, 4, and 5 wt%. A moderate mixing speed (up to 2,500 rpm) was employed at room temperature to avoid the destabilization of suspension. A satisfactory dispersion was accomplished using a Ragogna mixer specifically manufactured for FPInnovations by Custom Machinery Ltd. (Ontario, Canada) with speed up to 5,000 rpm. The prepared KF was then submerged into a water-ZnONPs emulsion that had been made beforehand. To prevent the nanoparticles from sedimenting, the KF was promptly immersed in the solution having ZnONPs for 60 min at 60 °C (moderate heat was applied to open up KF voids and allow ZnONPs to penetrate the KF cells). The treated KF layers were dried overnight at 80 °C in a conventional oven. ZnONPs powder was mixed with distilled water in serial percentages, which are tabulated in Table 2.

2.3. Composite preparation

The hand lay-up method was utilized to make a composite material formed into a stainless-steel mold with dimensions of 200 mm × 200 mm × 5 mm. Untreated and treated KF layers were compressed using Instron Universal Testing Machine (Model 5569) at 90 °C. Initially, the KF mat was positioned in the mold. Next, 2% of MEKP was added to UPE resin based

Table 2 Percentage of ZnONPs.

Amount of ZnONPs in distilled water (g/L)	Percentage of ZnONPs (wt%)
10	1
20	2
30	3
40	4
50	5

Table 3 Percentages of KF, UPE, and MEKP.

Kenaf (%)	UP (%)	MEKP (%)
10	88.2	1.8
20	78.4	1.6
30	68.6	1.4
40	58.8	1.2

on the UPE weight. This chemical item is utilizing in small quantities as a trigger for initiating the cross-linking of UP resin during the composites manufacturing process. Table 3 has been tabulated the percentages of KF, UPE, and MEKP. The UPE resin and MEKP mixture were then poured over the KF mat. The resin was distributed and impregnated using a hand roller. KF loadings were arranged in four different loadings (wight %) of 10, 20, 30, and 40 for both treated and untreated KF. The mold was covered on top and bottom of the mold with two stainless steel sheets. As indicated in Fig. 1, the molding was pressed using a Geotech Testing Machine and left at room temperature for 24 h to cure. Finally, the composites were cut into a 20 × 20 × 0.3 cm specimen using an electric saw.

3. Testing and characterization

3.1. Contact angle measurements

The contact angle is a prevalent method for measuring the surface wettability of the material. The contact angle was recorded by a Zeiss microscope which was equipped with a Goniometer Ocular. The fluid used to measure the contact angle was deionized water. 4 μL was the volume of the water droplet, and the measurement of the contact angle was repeated three times, and the average value was taken.

3.2. Water absorption

The samples were subjected to a water absorption test in accordance with ASTM D570-95. The samples were cut in the shape of a rectangular bar with a size of 30 × 5 × 2 mm (length × width × thickness). The samples were placed in water inside a closed bottle, and the experiment was conducted at ambient temperature. This experiment was conducted for ten weeks period with an interval of 1 week. This was followed by removing the samples from water, wiping them with a dry cloth, and weighing them on a digital balance to the nearest 0.001 g. This experiment was also performed on the UPE sample for comparison purposes. The percentage of water absorption was calculated following Equation (3).

$$Water\ \ absorption, \% = \frac{W1 - W0}{W0} \times 100\% \quad (1)$$

where w_0 = Weight of the dry sample, w_1 = Weight of the wet sample.

3.3. Tensile test

The tensile characteristics were depicted by Instron Universal Testing Machine (Model 5569), using a crosshead speed of 2 mm/min, while the sample size was 20 × 20 × 0.3 cm with a gauge length of 14 cm. The tensile strength and tensile modulus of the UPE/KF composites before and after surface treatment with zinc oxide nanoparticles were determined according to the ASTM D3039 (ASTM, 2014). Each composite was tested five times, and its average value is reported. Tensile strength and tensile modulus were calculated using Equations (1) and (2).

$$Tensile\ \ strength = \frac{Force}{Area} \quad (2)$$

$$Tensile\ \ Modulus = \frac{Stress}{Strain} \quad (3)$$

3.4. Transmission electron microscopy (TEM)

Transmission electron microscopy (TEM) was utilized to obtain the size, shape, and diameter of the nanoparticles (ZnONPs). TEM micrographs of the samples were obtained using Hitachi H7500 with a 70 kV accelerating voltage. The nanoparticles were dispersed initially in dry acetone solution, then placed the emulsion on carbon-coated 400 mesh copper grids. The sample then was left to dry at ambient temperature for around 5 min before the analysis. The obtained micrographs were then used to examine the structure of the nanoparticles.

3.5. Field Emission scanning electron microscopy (FESEM)

The size, shape, and diameter of the nanoparticles (ZnONPs) were determined using a Field Emission Scanning Electron Microscope (FESEM), a Carl Zeiss Supra 55VP, and a JEOL JSM-7600F. Platinum was used to cover the samples to prevent electron charging during the testing.

3.6. Scanning electron microscopy (SEM)

Using a JEOL JFC6460LA, the surface morphology of the tensile fractured surface of the prepared UPE/KF and UPE/KF-ZnONPs composites was examined. Before the test, the specimens were coated with a layer of platinum.

3.7. Atomic-Force microscopy (AFM)

Veeco di CP-II Atomic Force Microscope was used to examine the topography of the composites. The surface of the specimen was scanned in 6 points (two points at the center of the specimen, two points at perimeter of the specimen, and two points

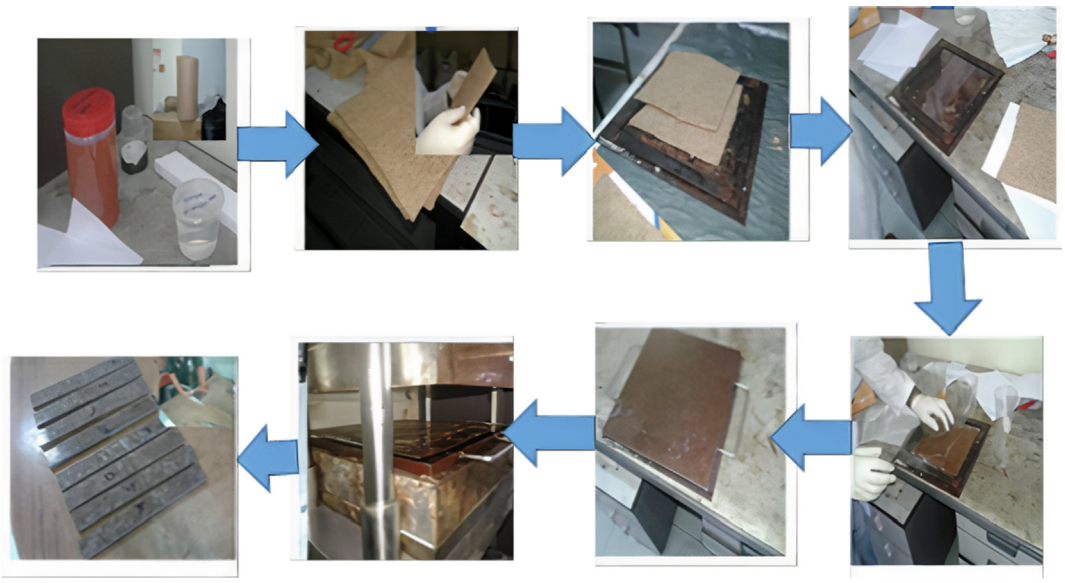

Fig. 1 Fabrication of composites.

at half distance between the center of the specimen and perimeter in contact mode with CONT20A-CP tips. 1 Hz scan rate and 256 × 256 resolution was maintained to obtain topography on a 5 × 5 μm scanning area.

3.8. X-ray diffraction (XRD) analysis

The microstructure and crystallinity of specimens were determined using a high-resolution X-ray Diffractometer (XRD) device model Phaser-D2 manufactured by Bruker company (X'Pert PRO), equipped with a monochromatic Cu-Ka radiation filter with wavelength = 0.154 nm. The experiment was run at room temperature with an angle range (2θ) from 5 to 70° at a scanning rate of 2°/min.

3.9. Fourier transform infrared spectroscopy (FT-IR)

Infrared spectra of the samples were obtained by a Perkin-Elmer Spectrum 65 Infrared Spectrometer with a scan number of 10 and resolutions of 4 cm^{-1}. All the composites were analyzed through an ATR technique and the wavenumber was in the range between 4000 and 500 cm^{-1}. In addition, FT-IR analysis was conducted to study the impacts of surface treatment of KF with ZnONPs on the chemical composition of KF after treatment.

4. Results and discussion

4.1. Contact angle (CA) measurement

The wettability properties of the treated KF-ZnONPs were characterized by measuring their contact angle. Fig. 2 shows the images of a water droplet on untreated KF and KF-ZnONPs with 1%, 2%, 3%, 4%, and 5% of ZnONPs. Understandably, KF is a hydrophilic material since it originated from natural fiber. It's hydrophilic nature has been reported by several research communities (Farahani et al., 2012). However, after treatment with ZnONPs, this hydrophilicity diminished. Treatment of KF with ZnONPs exhibited a hydrophobicity trend with a contact angle of 74.40° for the untreated KF. A linear increment in the contact angle is noted as treatment with ZnONPs from 1% to 5%. The contact angles were 80° for 1% ZnONPs, 82° for 2% ZnONPs, 85° for 3% ZnONPs, 95.2° for 4% ZnONPs, and 104.4° for 5% ZnONPs as shown in Fig. 2. These values were much higher than that of the untreated KF. The hydrophilic characteristics of the KF were found to be reduced by the ZnONPs.

The reason why surface treatment with ZnONPs did increase the hydrophobicity of KF is that the inorganic nanoparticles were integrated into the cell wall of KF and likely occupied the space (micropores) inside the cell wall that would have been accessible to water molecules, leading to a reduction in the hygroscopicity of the treated natural fibers (Donath et al., 2004; Hill, 2007). Furthermore, incorporation of the inorganic nanoparticles into cell walls reduces the capability of the cell wall to swell due to bulking, therefore improving the dimensional stability of the impregnated natural fibers. Therefore, only inorganic nanoparticles integrated into the cell wall are predicted to influence the hygroscopicity and dimensional stability of natural fibers significantly. In contrast, those deposited in the cell lumen are expected to have a negligible effect (Tshabalala et al., 2011).

On the other hand, the hydroxyl groups of cell wall components that are primarily responsible for moisture absorption may have been blocked during hydrolysis by creating hydrogen bonds with the inorganic nanoparticles, which may have contributed to the decreased hygroscopicity. In other words, the most notable functional group of natural material is the OH group which is well known to be taking part in extensive hydrogen bonding (Gao and McCarthy, 2008). This allows the ZnONPs to interact with the –OH–. Consequently, the –OH– group is fully occupied with no further available sites for interactions with moistures on the surface of the composite. Thus, the hydrophobicity of the composite is increased. Furthermore, the increase in contact angles may also be due to

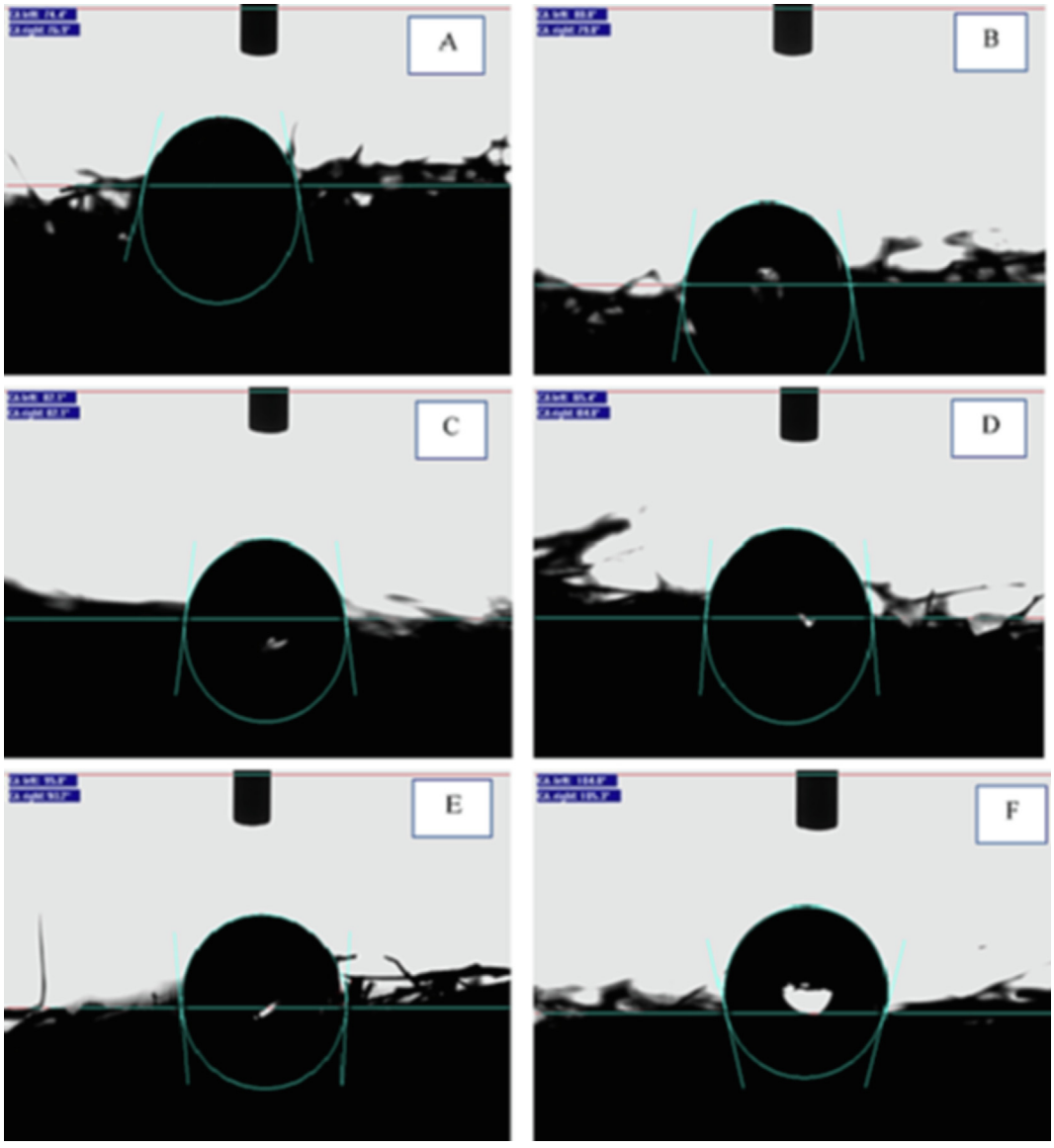

Fig. 2 Micrograph images of water dropping of KF with different percentage of ZnONPs. (a) untreated, (b) 1%, (c) 2%, (d) 3%, (e) 4%, (f) 5 wt% ZnONPs.

the presence of excess non-polar group ions on the surface of the composite brought by the treatment with ZnONPs.

4.2. Water absorption

We examined the effect of treating KF with ZnONPs on the water absorption of UPE/KF-ZnONPs composites. After measuring the contact angle of the UPE/KF composite after treatment with ZnONPs, the hydrophobicity has significantly increased by increasing ZnONPs concentration. Therefore, it is necessary to evaluate the water absorption of UPE/KF-ZnONPs composites before and after treatment, as shown in Fig. 3. In light of the overall outcome, it is clear that water absorption for the composites before treatment augmented as KF loadings increase. Immediate water absorption is observed in the specimens for up to 14 days before it begins to slow down. The hydrophilic property of natural fibers, activated by hydroxyl groups, is mainly responsible for this quick water absorption (Akil et al., 2011). This result corroborates the findings by Salem et al. that the augment in water absorption is attributable to the hydrophilic nature of the natural fibers and the high interface area between the fibers and matrix. Furthermore, the development of water transport routes inside the composites resulted in micro gaps between the fibers and the resin matrix (Salem et al., 2017).

The dry specimens absorb a greater quantity of water at the start of the immersion process, causing the fiber cell wall to inflate and rapidly acquire weight. After three weeks of testing, it was seen that all composites had attained equilibrium. Water absorption rose significantly more with increasing KF loadings. This increase was mainly due to the porous structure and hydrophilic characteristics of KF. However, water absorption decreased considerably as the ZnONPs treatment concentration was increased in all periods of immersion, indicating

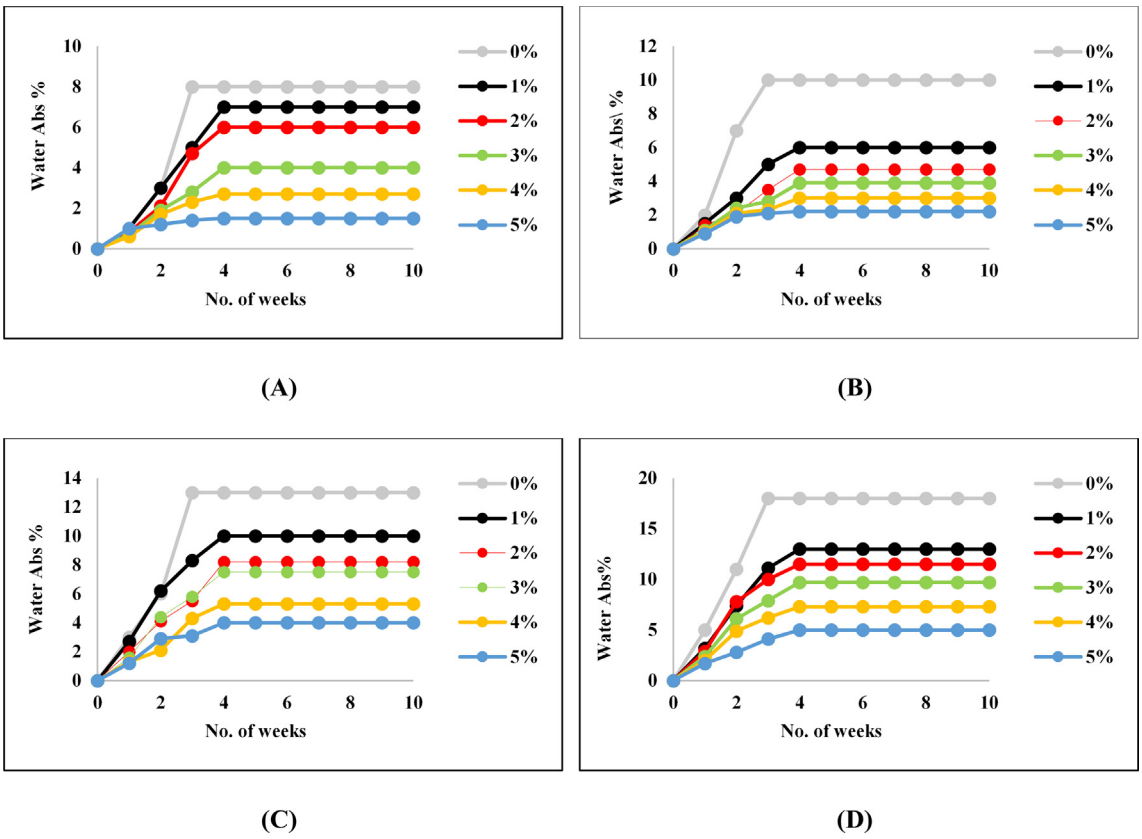

Fig. 3 water absorption test of (a) UPE/10 wt% KF- ZnONPs (b) UPE/20 wt% KF- ZnONPs, (c) UPE/30 wt% KF- ZnONPs and (d) UPE/40 wt% KF- ZnONPs after treatment with different concentrations of ZnONPs.

that the composite became hydrophobic and lacked affinity for high water absorption.

By comparing untreated and treated KF, untreated UPE/KF composites have a higher capacity for water absorption than treated UPE/KF-ZnONPs composites. The surface treatment with nanoparticles was expected to have a significant impact on the water absorption of UPE/KF-ZnONPs because the incorporation of inorganic nanoparticles into the micropore structure of the fiber cell walls could reduce the volume of microvoids within the fiber as well as minimize the formation of air bubbles throughout the composite manufacturing process. Additionally, inorganic nanoparticles block the hydroxyl group of cell wall components and act as a shield for fiber cell wall components, obstructing the pathway for a water molecule to enter matrices. This claim was also made by Li et al. (2017), who said that these inorganic nanoparticles were used to block the way for water infiltration, resulting in decreased water absorption by natural fibres. Table 4 illustrates the standard deviation of the water absorption according to the treatment %.

4.3. Mechanical properties

Fig. 4 demonstrates the influence of varying the proportion of zinc oxide nanoparticles on the tensile strength of UPE/ KF composites. As shown, treated KF reinforced-composites consistently outperformed untreated KF reinforced-composites at all different KF loadings and treatment with 1% and 2% ZnONPs. This observation is explained by the fact that treated KF with UPE exhibit superior interfacial adhesion to untreated KF, as illustrated in Fig. 5. Interfacial bonding between the fiber and matrix improves stress transfer between the components, allowing composites to reach their maximum strength (Hadjadj et al., 2016). However, the tensile strength of the UPE/KF-ZnONPs composites decreases at treatment with 3%, 4%, and 5% ZnONPs concentration at all different KF loadings. This is due to nanocomposites with a more significant nanoparticle weight fraction having a lower ultimate tensile stress, which is attributed to nanoparticle agglomeration at a higher nanoparticle weight fraction (Shokrieh et al., 2012). When the nanoparticle content of the nanocomposite exceeds a certain amount, particle agglomeration occurs, which serves as a barrier to stress transmission from the polymer matrix to the fiber, resulting in a decrease in mechanical performance in composites having a more significant proportion than 2% of inorganic nanoparticles, the same effect observed by Wang et al. (2011). The findings were consistent with those of Cosnita et al. (2017) that tensile stress decreased as nanoparticles loading increases. However, the dilemma of insufficient interfacial bonding between polymer matrix and fiber resulted in the ineffective transmission of stress between the polymer matrix and fiber, leading to a decline in tensile strength value (JA et al., 2016).

Additionally, Fig. 4 reveals that the impact strength of untreated UPE/KF composites rises with increasing KF loading. This assertion is consistent with the broad observation

Table 4 The standard deviation of the water absorption.

Sample	Water absorption %	SD
UPE/10 wt% KF- 0% ZnONPs	8	1.34
UPE/10 wt% KF- 1% ZnONPs	7	1.12
UPE/10 wt% KF- 2% ZnONPs	6	1.37
UPE/10 wt% KF- 3% ZnONPs	4	0.92
UPE/10 wt% KF- 4% ZnONPs	2.7	0.77
UPE/10 wt% KF- 5% ZnONPs	1.5	0.43
UPE/20 wt% KF- 0% ZnONPs	10.2	1.97
UPE/20 wt% KF- 1% ZnONPs	6	1.51
UPE/20 wt% KF- 2% ZnONPs	4.7	1.33
UPE/20 wt% KF- 3% ZnONPs	3.9	1.09
UPE/20 wt% KF- 4% ZnONPs	3	1.05
UPE/20 wt% KF- 5% ZnONPs	2.2	0.98
UPE/30 wt% KF- 0% ZnONPs	13.4	2.09
UPE/30 wt% KF- 1% ZnONPs	10	1.86
UPE/30 wt% KF- 2% ZnONPs	8.2	1.67
UPE/30 wt% KF- 3% ZnONPs	7.5	1.71
UPE/30 wt% KF- 4% ZnONPs	5.3	1.57
UPE/30 wt% KF- 5% ZnONPs	4	1.39
UPE/40 wt% KF- 0% ZnONPs	17.9	2.79
UPE/40 wt% KF- 1% ZnONPs	13	2.30
UPE/40 wt% KF- 2% ZnONPs	11.5	2.02
UPE/40 wt% KF- 3% ZnONPs	9.7	1.83
UPE/40 wt% KF- 4% ZnONPs	7.3	1.51
UPE/40 wt% KF- 5% ZnONPs	5	1.23

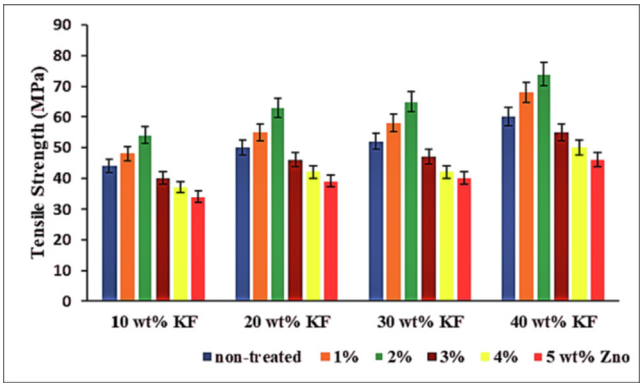

Fig. 4 Tensile strength of the fabricated treated and untreated UPE/KF composites.

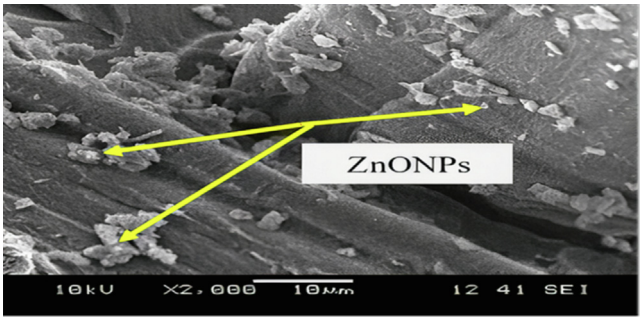

Fig. 5 SEM micrographs of UPE/KF-ZnONPs composite treated with 2% ZnONPs.

that the mechanical strength of polymer composites increases with increasing KF loadings up to specific loading before its lowering (Mohammed et al., 2018). In this investigation, the tensile strength rose dramatically at 30% KF loading incorporation. The optimal loading of KF was 40 wt% KF loading inclusions with a slight increase in tensile strength. Additional loadings of KF at 45% loadings diminished the tensile strength of the UPE/KF composites. The explanation for this is that the resin matrix is insufficient to wet the reinforcement KF effectively. Insufficient fiber saturation can trigger inadequate interfacial bonding strength. It was consistent with the findings of Salman et al. (Salman et al., 2016), who identified that the composite comprising 40% KF loadings exhibited the largest tensile strength value before reducing with increased KF loadings. The matrix could not adequately wet the fiber at higher KF loadings (45 wt% and 50%). Such a condition impairs the capability of the matrix to convey the load to the reinforcement fiber. For comparison purposes, the percentage difference in the tensile strength of UPE/KF composites before and after treatment of KF with different percentages of ZnONPs is tabulated in Table 5. It was found that an increasing rate of ZnONPs has a tangible impact on the increments in the tensile strength up to treatment with 2% of ZnONPs. However, values greater than 2% caused a reduction in tensile strength.

The effect of varying the percentage of ZnONPs on the tensile modulus of different KF loadings UPE/ KF composites is demonstrated in Fig. 6. It reveals that the treated KF composites have a higher tensile modulus at 2% ZnONPs than untreated KF composites. It was explained as treatment with ZnONPs entered into the configurations of KF and the kenaf polymer interface. This intrusion resulted in an improvement in mechanical properties. The topic of polymer adhesion to natural materials has long been a source of worry for researchers working in this field, as the compatibility of the components of these materials has caused severe issues. However, significant adhesion between KF and matrix was established, most likely owing to the presence of the ZnO nanoparticles, which enhances the molecular interaction between KF and polymer matrix (Mohammed et al., 2018; Mohammed et al., 2019).

The tensile modulus result revealed that as the proportion of ZnONPs was raised above 2%, the tensile modulus started to decline. The reason behind this is that the higher percentage of nanoparticles tends to agglomerate. The agglomeration of ZnONPs will lead to more interactions between the nanoparticles instead of the nanoparticles with KF, as seen in Fig. 7. Thus, it can be observed that ZnONPs clusters have been loaded onto the surface of the UPE/KF-ZnONPs composite, forming a more obvious micro nanostructure. As a result, the reduction in modulus occurs. Fu et al. (Fu et al., 2008) investigated the impacts of particle size, particle/matrix adhesion, and particle loading of nanoparticles on rigidity, hardness, and strength of nanocomposites. According to the researchers, all the three variables, notably particle/matrix adhesion, have a substantial impact on composite strength and toughness.

As seen in Fig. 6, the tensile modulus of untreated and treated KF composites augmented as the loading of KF rose. The explanation for this is that when the KF loadings rise, the quantity of cellulosic material in the composites increases, increasing the stiffness of the UPE composites (Mohammed

Table 5 The percentage difference in tensile strength before and after treatment with ZnONPs.

Sample	Tensile strength (MPa)	Increment (%)	Decrement (%)
10% KF loadings before/after treatment with 1% ZnONPs	44/48	8.3	–
10% KF loadings before/after treatment with 2% ZnONPs	44/54	18.5	–
10% KF loadings before/after treatment with 3% ZnONPs	44/40		10.0
10% KF loadings before/after treatment with 4% ZnONPs	44/37		18.9
10% KF loadings before/after treatment with 5% ZnONPs	44/34		29.4
20% KF loadings before/after treatment with 1% ZnONPs	50/55	9.1	–
20% KF loadings before/after treatment with 2% ZnONPs	50/63	20.6	–
20% KF loadings before/after treatment with 3% ZnONPs	50/46	–	8.7
20% KF loadings before/after treatment with 4% ZnONPs	50/42	–	19.0
20% KF loadings before/after treatment with 5% ZnONPs	50/39	–	28.2
30% KF loadings before/after treatment with 1% ZnONPs	52/58	10.3	–
30% KF loadings before/after treatment with 2% ZnONPs	52/65	20.0	–
30% KF loadings before/after treatment with 3% ZnONPs	52/47	–	10.6
30% KF loadings before/after treatment with 4% ZnONPs	52/42	–	23.8
30% KF loadings before/after treatment with 5% ZnONPs	52/40	–	−30.0
40% KF loadings before/after treatment with 1% ZnONPs	60/68	11.8	–
40% KF loadings before/after treatment with 2% ZnONPs	60/74	18.9	–
40% KF loadings before/after treatment with 3% ZnONPs	60/55	–	−9.1
40% KF loadings before/after treatment with 4% ZnONPs	60/50	–	−20.0
40% KF loadings before/after treatment with 5% ZnONPs	60/46	–	−30.3

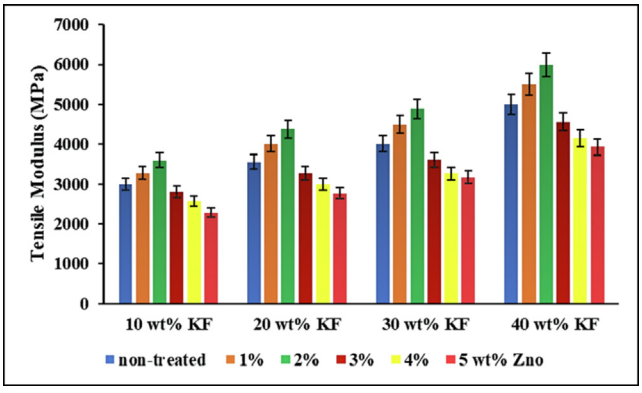

Fig. 6 The tensile modules of the treated and untreated UPE/KF composites.

et al., 2018; Mohammed et al., 2019). For the sake of comparison, Table 6 shows a percentage difference in the UPE / KF composite tensile modulus before and after KF treatment with different ZnONPs percentages. The increasing percentage of ZnONPs was found to substantially impact increases in the tensile modulus up to 2% of ZnONPs treatment. However, higher than 2% led to a descend in the tensile modulus. Based on these findings, it can be inferred that the mechanical properties were improved at 40% loadings of KF, but unfortunately, it comes with higher water absorption expenses. As fiber volume rises, the rate of moisture absorption increases proportionately. Therefore, when a natural fiber composite is used outdoors, the fiber content should be kept under control to achieve the required strength. This is to reduce moisture absorption and enhance the durability of composites (Azwa et al., 2013). The results so far obtained allow concluding that inorganic nanoparticles ZnONPs and fiber loadings have a synergistic impact on the mechanical characteristics of these composites.

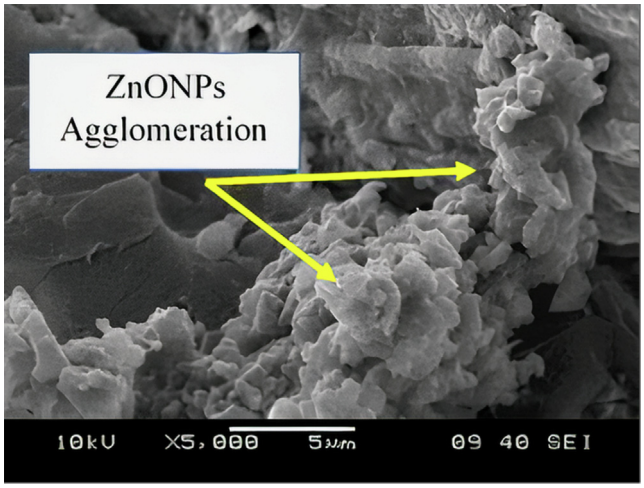

Fig. 7 SEM micrographs of UPE/KF-ZnONPs composite treated with 5% ZnONPs.

4.4. TEM and FESEM of zinc oxide nanoparticles

TEM and FESEM morphology were conducted to confirm the nature of the nanoparticles (ZnONPs). Typical TEM and FESEM micrographs of the nanoparticles ZnONPs are illustrated in Fig. 8 and Fig. 9, respectively. Generally, TEM images revealed that the average diameter and length of ZnONPs nanoparticles were around 25 nm to 50 nm and 100 nm to 200 nm, respectively. This result demonstrates that the morphological structure of the ZnONPs is a rod-like shape in hexagonal form. These results were found in agreement with those provided by the FESEM results. In addition, the average size of nanoparticles was found to be around 45 nm.

Table 6 The percentage difference in tensile modulus before and after treatment with ZnONPs.

Sample	Tensile modulus (MPa)	Increment (%)	Decrement (%)
10% KF loadings before/after treatment with 1% ZnONPs	3000/3284	8.6	–
10% KF loadings before/after treatment with 2% ZnONPs	3000/3599	16.6	–
10% KF loadings before/after treatment with 3% ZnONPs	3000/2809	–	6.8
10% KF loadings before/after treatment with 4% ZnONPs	3000/2578	–	16.4
10% KF loadings before/after treatment with 5% ZnONPs	3000/2292	–	30.9.4
20% KF loadings before/after treatment with 1% ZnONPs	3562/4002	10.9	–
20% KF loadings before/after treatment with 2% ZnONPs	3562/4376	18.6	–
20% KF loadings before/after treatment with 3% ZnONPs	3562/3279	–	8.6
20% KF loadings before/after treatment with 4% ZnONPs	3562/3001	–	18.6
20% KF loadings before/after treatment with 5% ZnONPs	3562/2771	–	28.5
30% KF loadings before/after treatment with 1% ZnONPs	4003/4489	10.8	–
30% KF loadings before/after treatment with 2% ZnONPs	4003/4878	17.9	–
30% KF loadings before/after treatment with 3% ZnONPs	4003/3609	–	10.9
30% KF loadings before/after treatment with 4% ZnONPs	4003/3270	–	22.4
30% KF loadings before/after treatment with 5% ZnONPs	4003/3182	–	25.8
40% KF loadings before/after treatment with 1% ZnONPs	4993/5512	9.4	–
40% KF loadings before/after treatment with 2% ZnONPs	4993/5986	16.6	–
40% KF loadings before/after treatment with 3% ZnONPs	4993/4557	–	9.6
40% KF loadings before/after treatment with 4% ZnONPs	4993/4142	–	20.5
40% KF loadings before/after treatment with 5% ZnONPs	4993/3926	–	27.1

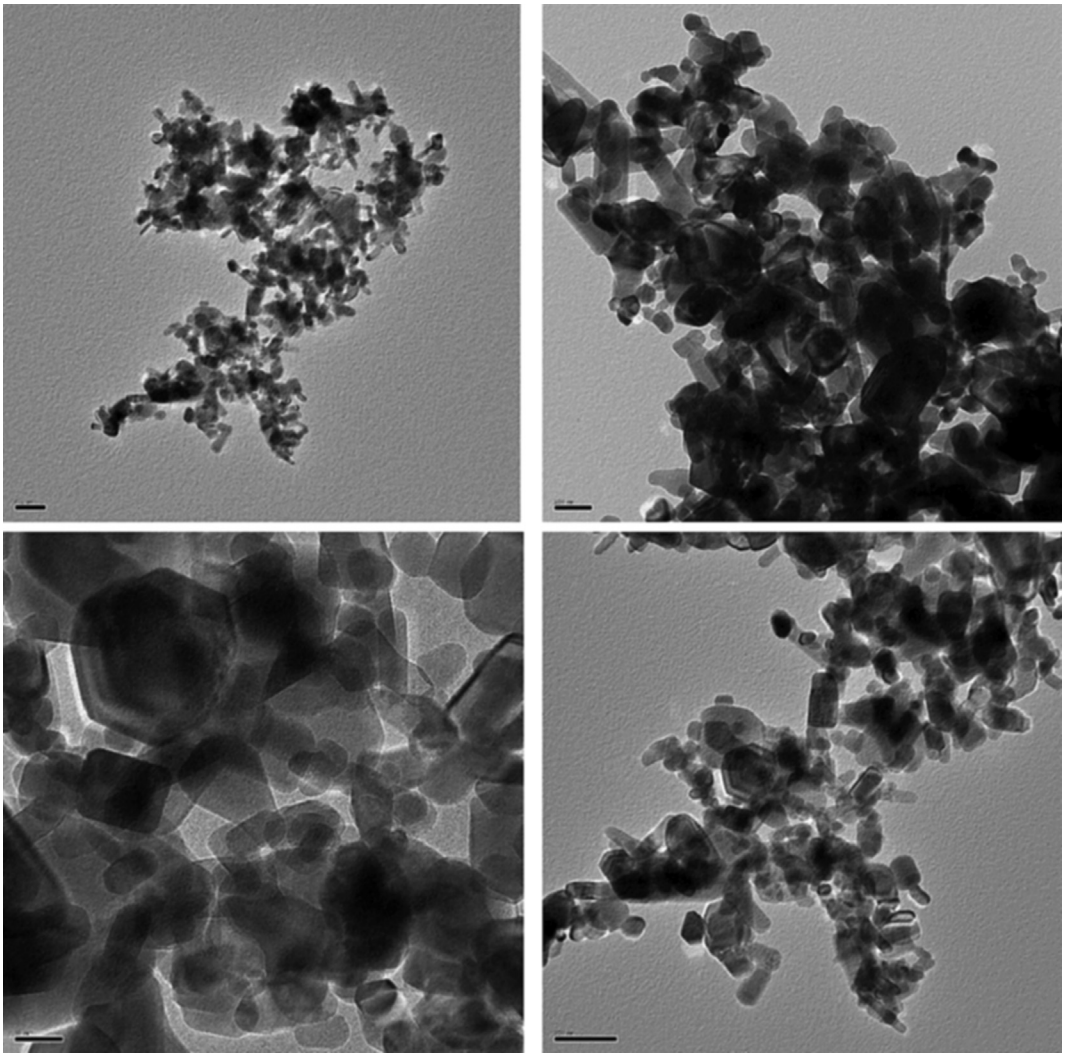

Fig. 8 TEM micrographs of ZnONPs.

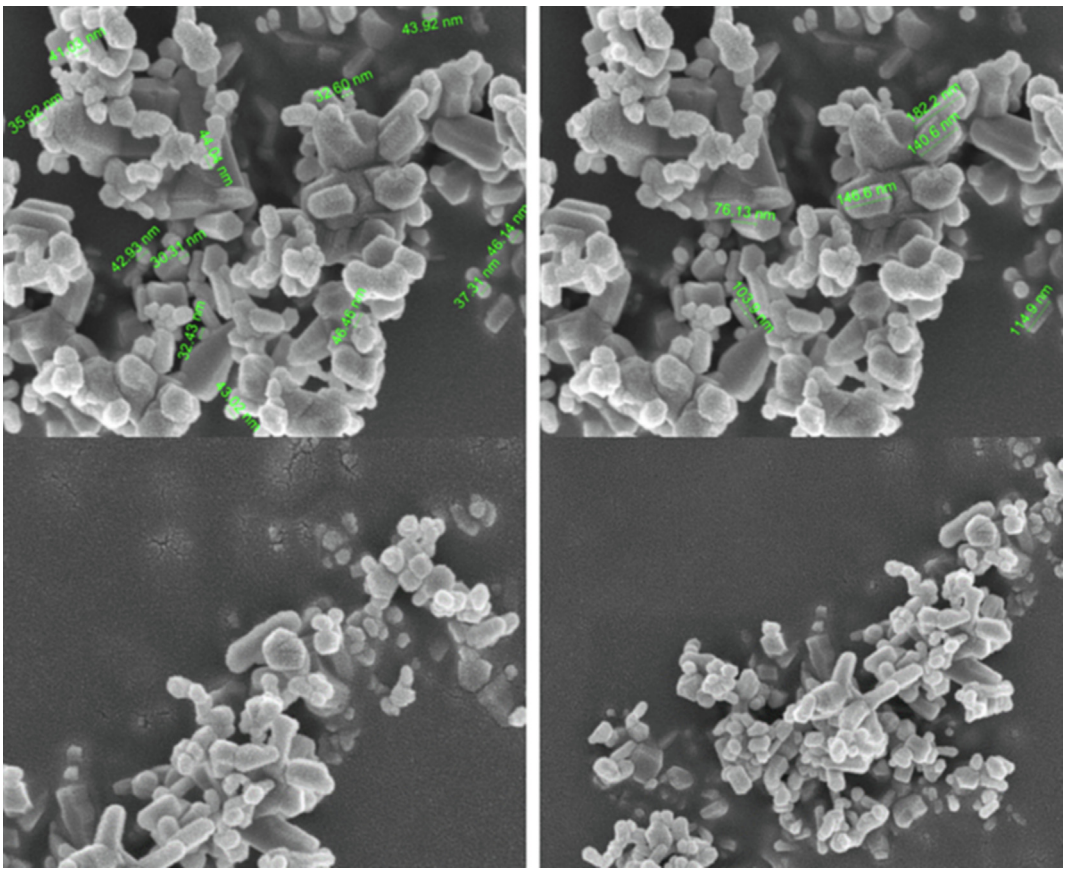

Fig. 9 FESEM micrographs of ZnONPs.

4.5. Surface morphology

Fig. 10 (a) and (b) display the microscopic photographs of the treated UPE/KF- ZnONPs with 1% and 5% of ZnONPs, respectively, at 5000× magnifications. As demonstrated, the nanoparticles were homogeneous and scattered evenly at 1% ZnONPs. On the other hand, the pattern of dispersion was different for considerably higher percentages, as for 5% ZnONPs, and was less consistent than for lower percentages, such as 1% ZnONPs. As shown in Fig. 10 (b), higher contents of ZnONPs showed the presence of agglomeration as nanoparticles have a high surface area and high surface energy. As a result, dispersing them equally on the KF surface is difficult (Pukánszky and Fekete, 1999). Fig. 10 (a) shows that treated KF has a rough and unblemished fiber surface. Hence, it will contribute to the improvement in the mechanical characteristics of the treated UPE/KF- ZnONPs, as depicted in Fig. 4 (Mohammed et al., 2019).

In comparison to the treated KF, impurities of the nonfibrous matter remain on the surface of the untreated KF. For example, Fig. 10 (c) and (d) of UPE/ 10 wt% KF and UPE/ 30 wt% KF composites show a prominent gap between the fiber and the matrix in untreated KF composites. This indicates impaired interfacial bonding between untreated KF and UP matrix resin, resulting in inferior tensile characteristics. Lai et al. (2016) presented a similar observation with a similar morphology appearance.

The mechanical characteristics of polymer matrix composites are impacted by the nature and structure of the fiber–matrix interface (Hadjadj et al., 2016). Fig. 10 (e) and (d) depict the interfacial bonding between KF and polymer matrix via microscopic photographs of cracked surfaces of treated and untreated KF composites. There were several fiber breakages between the treated KF and the UPE matrix, no fibers were pulling out, and fewer holes were observed. This finding suggests that UPE clings to the KF, enhancing the capability of composites to carry the load when force was exerted. However, compared to the untreated KF composites in Fig. 10 (d), cavities between the fibers and matrix were observed, indicating an inadequate bonding between the fibers and polymer matrix that exacerbates the reduced capability of composites to bear the smashing once the exertion of force.

4.6. Atomic force microscopy (AFM) of the fibers

The topological properties of the untreated and treated KF were also investigated using the AFM under the ambient environment. The two-dimension AFM micrographs of the untreated KF and treated KF-ZnONPs with 1, 2, 3, 4, and 5% ZnONPs are shown in Fig. 11 (a), (b), (c), (d), (e) and (f) respectively. Micrographs allowed for a good grasp of the topographical changes seen in the KF. According to the findings, the untreated KF showed a smooth surface. However, after treatment with ZnONPs, the surface roughness gradually augmented as ZnONPs content increase, indicating that more ZnONPs resided at the surfaces of the KF as more ZnONPs nanoparticles were embedded (Xiong et al., 2004).

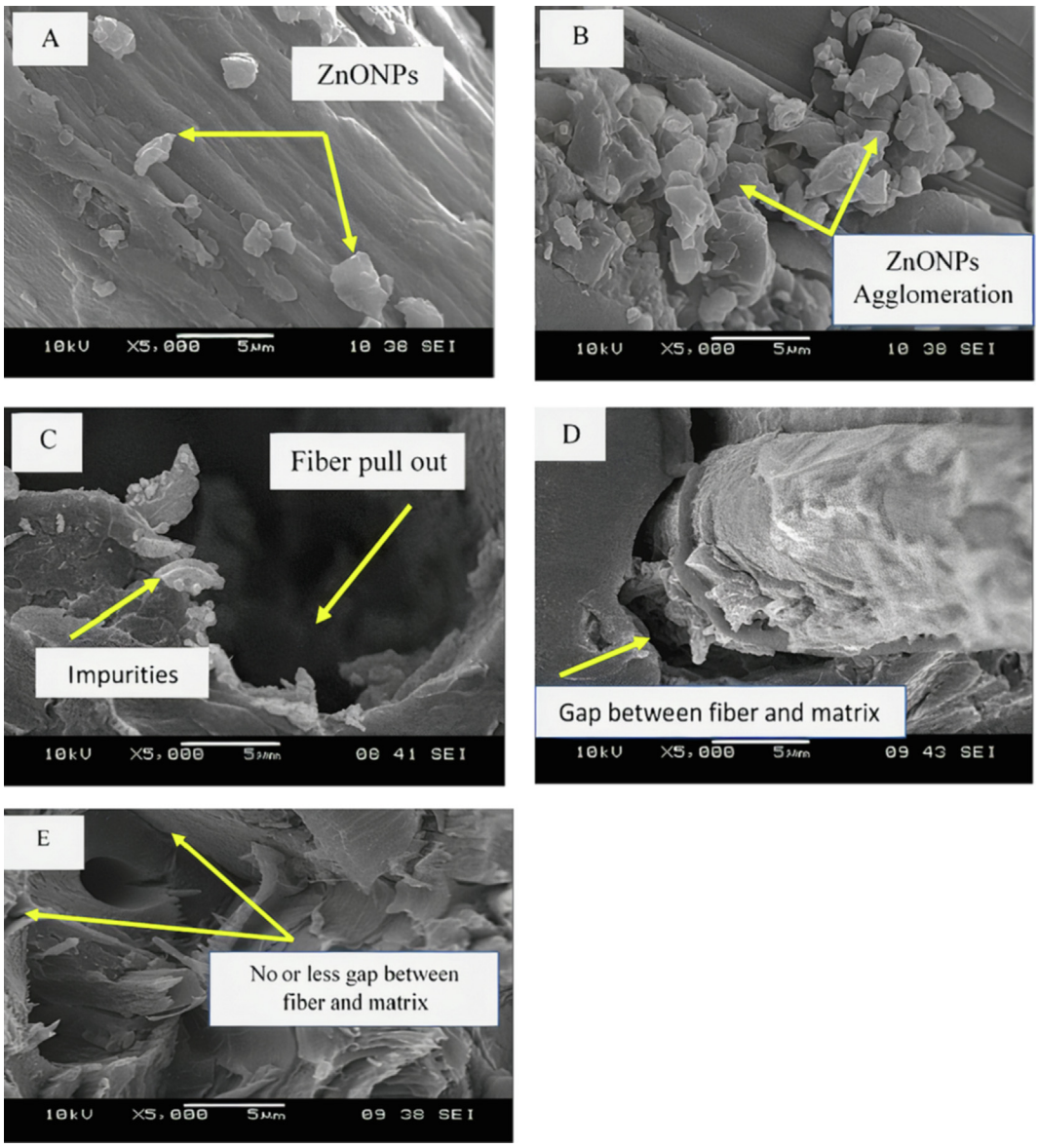

Fig. 10 SEM micrographs of (a) UPE/KF-1% ZnONPs, (b) UPE/KF-5% ZnONPs, (c) UPE/ 10 wt% KF, (d) UPE/ 30 wt% KF, (e) UPE/KF- 2% ZnONPs composite.

From the Fig. 11, bright areas represent increased adhesion forces between the tip and fiber, while the dark areas represent decreased adhesion forces. There were numerous large brighter areas in the AFM adhesion image of the untreated KF. The adhesion forces were distributed more uniformly on the surface of KF-ZnONPs than on untreated KF. After the treatment with ZnONPs, the adhesion force between the fiber and AFM tip was reduced because the roughness of the surface increased. This force is a combination of van der Waals and capillary forces (Butt et al., 2005). This revealed that the presence of ZnO NPs inorganic nanoparticles at the surface of the fiber causes the surface roughness to grow progressively. The investigation by Liang et al. (2014) confirms this out.

Atomic force microscope images (AFM) revealed that the ZnONPs nanoparticles could successfully produce nano-level roughness, which was advantageous to the hydrophobic characteristics. A rough surface of the KF can increase UPE-KF adhesion by creating good interlocking with the surface of the UPE. This is demonstrated by the tensile modulus composite, which exhibits increased strength as the interfacial bonding between KF and UPE matrix increased (Liang et al., 2014). However, as the content of ZnO NPs nanoparticle increases, poor interfacial adhesion can be observed as a result of the encouragement of a wide debonding gap between fiber and polyester, as well as influence on the sample surface physical and topology that we were preferred to stop at 5% concentration of ZnONPs nanoparticles. It is critical to note that an increase in the mechanical characteristics of polymeric composites can be attributed to the compatibility of the fiber and matrix, as discussed in the section on mechanical properties above. The high surface area interaction from the ZnONPs, UPE, and KF causes an increase in interfacial adhesions

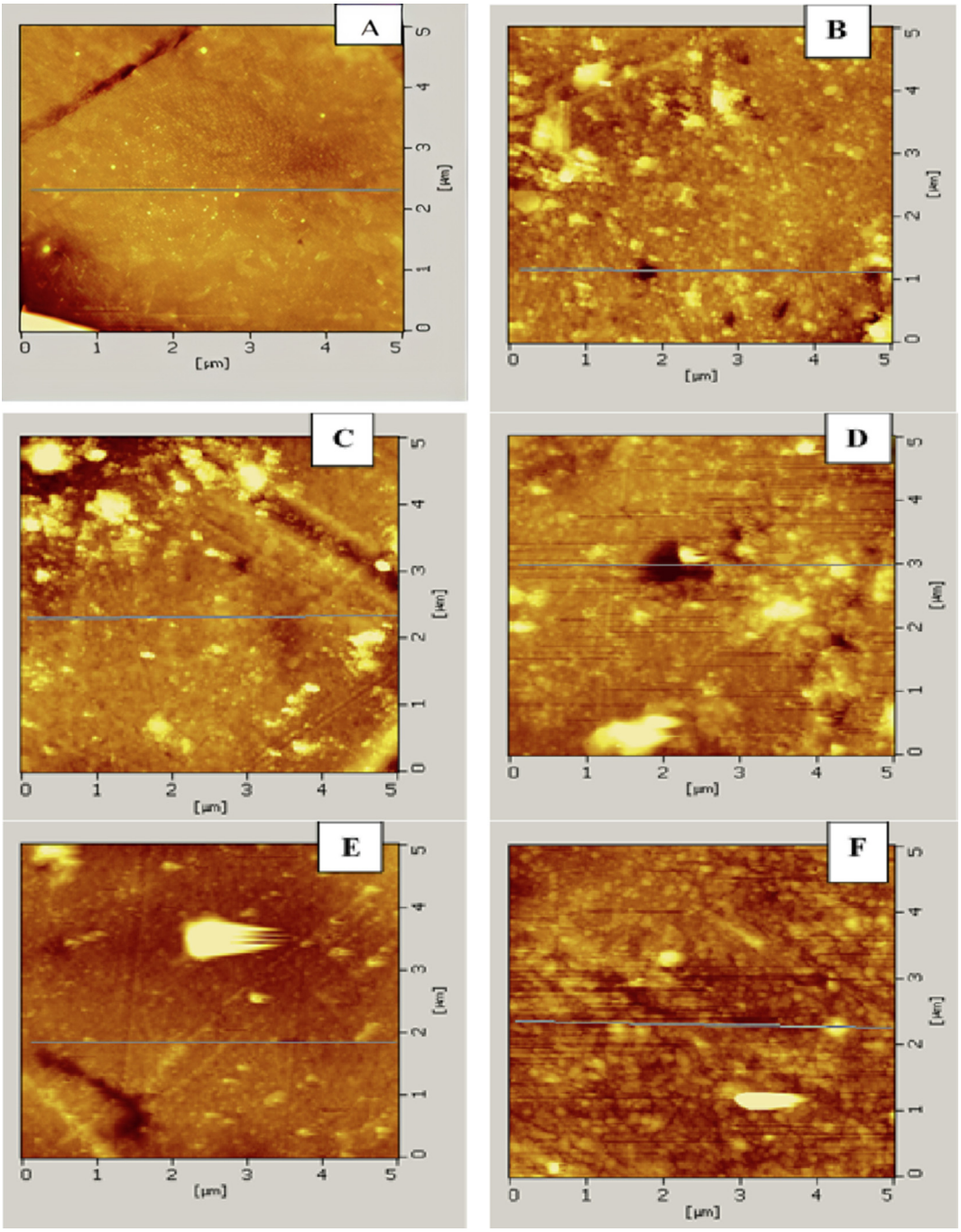

Fig. 11 AFM images (a) untreated KF, (b) KF- 1% ZnONPs, (c) KF- 2% ZnONPs, (d) KF- 3% ZnONPs, (e) KF- 4% ZnONPs, (f) KF- 5% ZnONPs.

and, therefore, a more homogenous surface of the composite. These findings are consistent with the outcomes of the mechanical characteristics, which revealed an augment in compression resistance due to the formation of a more compact interface and a high rough surface.

4.7. (X-RD) crystallinity of the UPE/KF-ZnONPs

XRD analysis was utilized to analyse the crystalline structure of the composites and the formation of a new crystalline compound due to the addition of ZnONPs nanoparticles. The comparison of the composite diffractograms of ZnONPs, untreated UPE/KF, and treated UPE/KF-ZnONPs composites is presented in Fig. 12. According to the XRD results, ZnONPs exhibited diffraction peaks at 2θ in the planes of (100), (002), (101), (102), (110), (103), and (112), respectively. These planes typically represent the hexagonal Wurtzite structure (Kulyk et al., 2010).

However, new peaks emerged in the composite architectures evidencing the presence of ZnONPs, particularly in the UPE/KF-ZnONPs composites with 5% ZnONPs concentrations which revealed the formation of new peaks at 2θ = 31.

85°, 34.55°, and 36.35°. These peaks can be ascribed to (1 0 0), (0 0 2), and (1 0 1) ZnO crystal planes, respectively (Sui et al., 2006). This demonstrates the presence of ZnONPs along its c-axis on the KF surface. Peaks located at 46.98°, 56.33°, and 62.19° correspond to crystal planes (1 0 2), (1 1 0), and (1 0 3), respectively, and indicate the formation of hexagonal wurtzite ZnO structure (d'Água et al., 2018). Similar research performed by Arfaoui et al. (2017) found that the new peaks equally showed a new functional group as a marker of chemical interaction by adding the ZnONPs nanoparticles. This new chemistry indicated that specific interactions between nanoparticles and the composite were formed. The amorphous UPE/KF composite peak is present in all six diffractograms at $2\theta \sim 22.23°$. However, a slight reduction in the intensity of the amorphous peak simultaneously with a new crystalline peak has developed at 2θ = 15.54°, 31.85°, 34.55°, and 36.35°. These findings indicate the emergence of a new diffraction peak in the UPE/KF composite, which is most likely the consequence of nanoparticles acting as nucleation centers in the KF. Therefore, it can be inferred that composites having ZnONPs nanoparticles may produce novel crystalline, water-repellent compounds that improve the ordering at the interface area. This aspect is essential for the dimensional stability of a composite that contains KF as a hydrophilic component.

4.8. FTIR spectra analysis

The FTIR spectra of untreated and treated KF with 1%, 2%, 3%, 4%, and 5% ZnONPs at various fiber loadings are shown in Fig. 13 (a), (b), (c), (d), (e), and (f), respectively. It has been found that the FTIR spectra for the untreated samples exhibit intensity bands in the regions 3340 cm^{-1}, 1732 cm^{-1}, 2800–3000 cm^{-1}, 1640, and 1000 cm^{-1}–1245 cm^{-1} due to O—H stretching vibration, C═O stretching vibration, C—H stretching vibration, C═C stretching vibration, and C—O—C stretching vibration, correspondingly (Li et al., 2011). These absorbance bands are caused by hydroxyl groups in cellulose, acetyl ester carbonyl groups in hemicellulose, and carbonyl aldehydes and aromatic compounds in lignin.

The FTIR spectra of the treated KF samples have almost identical functional peaks to that of untreated KF. However, peak No.1 at wave number 3340 cm^{-1} in Fig. 13 (a), (b), (c), (d), (e) and (f), the intensities decreased. This is most likely due to the use of ZnONPs nanoparticles in the treatment, which blocks hydroxyl (OH) functional groups responsible for moisture absorption. This OH stretching is related to hydroxyl (OH) functional groups in lignocellulose natural fibers made up of cellulose, hemicellulose, lignin, wax, and pectin. The peak for untreated KF has a broader intensity, indicating greater hydroxyl OH functional group content (Nosbi et al., 2011). The intensities decreased at wave numbers between 2800 and 3000 cm^{-1} (peak No. 2) attributable to the nano treatment with ZnONPs nanoparticles. The intensities of peak No. 3 decreased because of the treatment (Ding et al., 2012; Pandey and Pitman, 2003).

As a result of the treatment, the intensities of the peak at about 1640 cm^{-1} (peak No. 4) were reduced. This peak has been attributed to an aromatic skeletal vibration in lignin (C═C stretch) (Pandey and Pitman, 2003; Bak et al., 2012; Papadopoulos and Mantanis, 2011). Additionally, as ZnONPs concentration rose, there was a reduction in the peak at

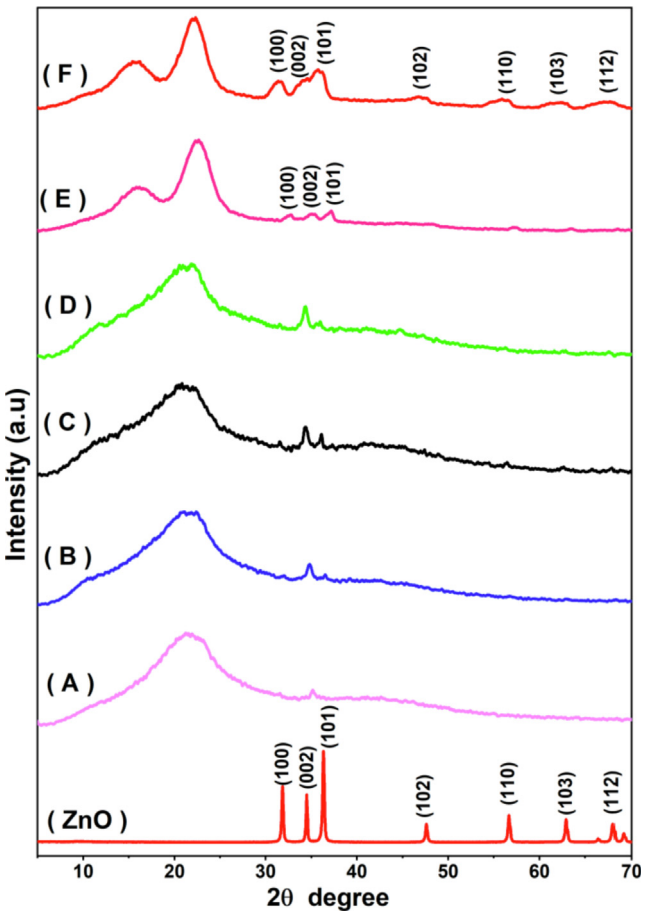

Fig. 12 XRD pattern of ZnO nanoparticles, and (a) untreated UPE/KF, (b) UPE/KF- 1% ZnONPs, (c) UPE/KF- 2% ZnONPs, (d) UPE/KF- 3% ZnONPs, (e) UPE/KF- 4% ZnONPs, (f) UPE/KF- 5% ZnONPs.

1432 cm^{-1} (peak No. 5), which appeared to be associated with C—H deformation in lignin (Pandey et al., 2012). The bands of peaks 4 and 5 are transformed into an association of three bands at about 1590, 1495, and 1451 cm^{-1} with 5% (wt%) ZnONPs nanoparticles, demonstrating a chemical interaction between KF, UPE, and probably the inorganic nanoparticles. Furthermore, the band at 1030 cm^{-1} was changed into an association of two bands at about 1124 and 1069 cm^{-1}, indicating a potential interaction between the components of the composite.

The intensity of the peak at wave number 1328 cm^{-1} (peak No. 6), which has been related to C—H (CH3 bonding), and also, the intensity of the prominent peak (No. 7) between 1000 and 1245 cm^{-1}, which has been related to C—O stretching and C═O deformation in lignin and xylan for the syringyl ring decreased in the treated samples compared to that of the untreated KF (Ding et al., 2012; Pandey and Pitman, 2003). This peak (No.7) elucidates that hemicellulose and lignin are present in the untreated and treated KF (Sun et al., 2004).

FTIR analysis disclosed an increase in the number of the band after surface treatment with ZnONPs nanoparticles, suggesting new chemical interaction between the polymeric composite components UPE, KF, and ZnONPs nanoparticles. These findings corroborate the mechanical test results. Never-

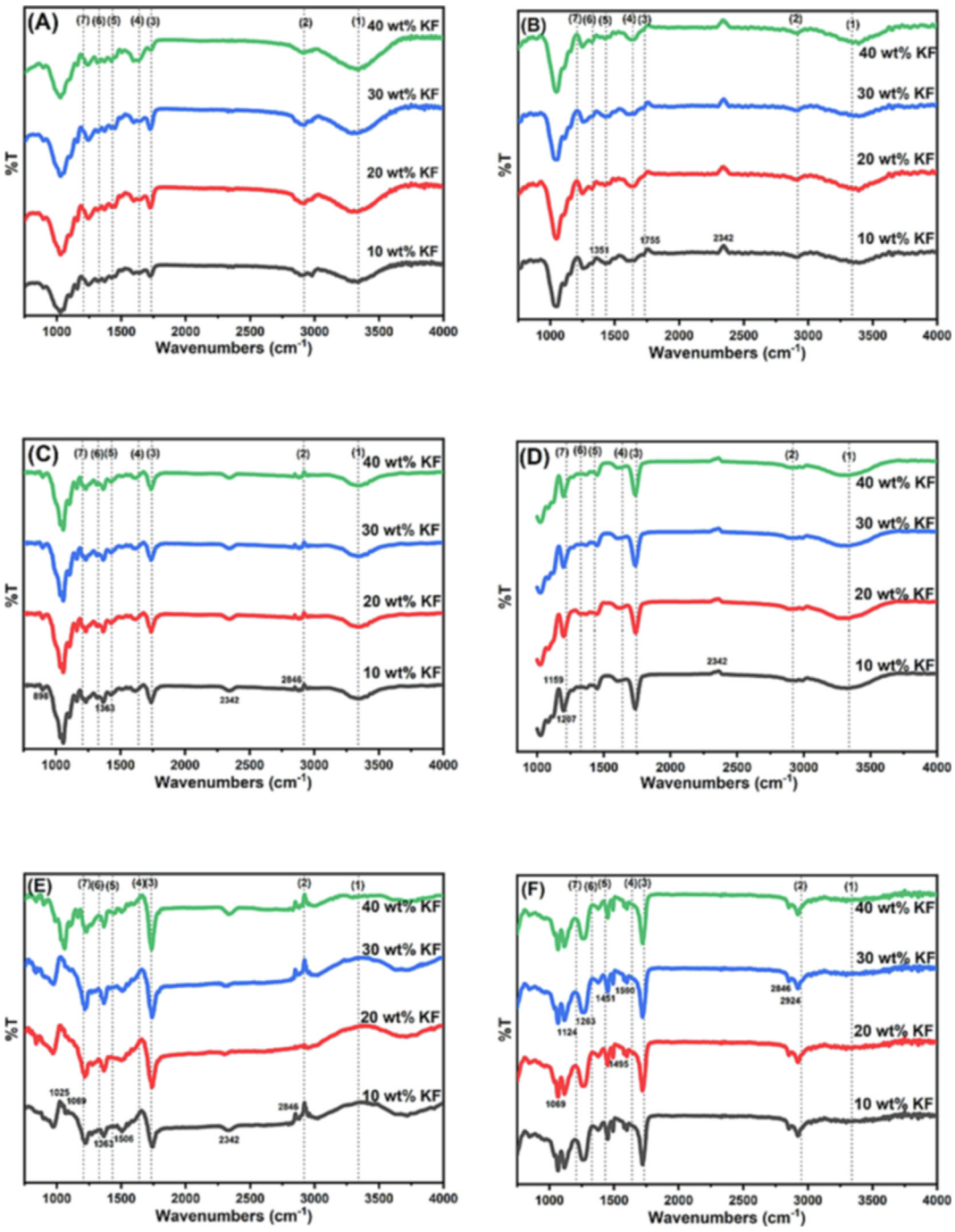

Fig. 13 FTIR spectra of (a) untreated UPE/KF, (b) UPE/KF- 1% ZnONPs, (c) UPE/KF- 2% ZnONPs, (d) UPE/KF-3% ZnONPs, (e) UPE/KF- 4% ZnONPs, (f) UPE/KF- 5% ZnONPs.

theless, other authors have attributed ZnO to additional peaks, including 2865–2971 cm^{-1} (Traistaru et al., 2012), 3419 cm^{-1} (AbdElhady, 2012), and 3409 cm^{-1} (Salehi et al., 2010).

5. Conclusion

The impacts of surface treatment with zinc oxide nanoparticles on water absorption and tensile strength characteristics of KF-reinforced UPE composites were evaluated. SEM and AFM were used to analyse the morphologies of the tensile fracture surface and fibers. FTIR was also used to investigate functional group distinctions for both untreated and treated KF. Based on the findings and experimental data, the following conclusions are drawn:

1. The addition of ZnONPs in the composites exhibited a hydrophobicity trend. As the ZnONPs were added from 1% to 5%, a linear increment in contact angle was noted, 80° for the 1% ZnONPs and up to 104.4° for the 5% ZnONPs.
2. Water absorption is more remarkable in untreated KF- reinforced UPE composites than in treated KF- reinforced UPE composites due to the existence of more hydroxyl groups.

3. Treated KF-reinforced UPE composites exhibit increased tensile strength due to the enhanced interfacial bonding between the treated KF and UPE matrix compared to untreated KF-reinforced UPE composites.
4. Compared to untreated KF, treated KF had a rough surface, no fiber pull out, and fewer gaps between the fibers and matrix. Additionally, ZnONPs exhibit agglomeration at higher concentrations of 3%, 4%, and 5% of ZnONPs because nanoparticles have a higher surface area to volume fraction and high surface energy (SEM micrographs).
5. Surface treatment was successful by ZnONPs nanoparticles, and the roughness of KF was further improved by adding ZnONPs nanoparticles (SEM and AFM images).
6. The results show that adding 2 wt% ZnONPs nanoparticles and 40 (wt%) of KF loading led to a good hydrophobicity and better compatibility between fiber and polymer matrix. As a result, we recommend these composites for outdoor applications such as paving slabs, park carpets, floor decking, and for use in wet working environments.

Declaration of Competing Interest

The authors declare that they have no known competing financial interests or personal relationships that could have appeared to influence the work reported in this paper.

Acknowledgement

The authors like to express their appreciation to Malaysia's Lembaga Kenaf Tembakau Negara (LKTN) for delivering raw materials and support during this study. The authors also acknowledge the Faculty of Chemical Engineering Technology, Universiti Malaysia Perlis (UniMAP), for providing the necessary tools and practical assistance. Finally, the authors like to express their appreciation for the constructive conversations and contributions made to the project by the UniMAP team.

References

AbdElhady, M.M., 2012. Preparation and characterization of chitosan/zinc oxide nanoparticles for imparting antimicrobial and UV protection to cotton fabric. Int. J. Carbohydrate Chem. 2012.

Akil, H., Omar, M.F., Mazuki, A.M., Safiee, S.Z.A.M., Ishak, Z.M., Bakar, A.A., 2011. Kenaf fiber reinforced composites: A review. Mater. Des. 32 (8–9), 4107–4121.

Arfaoui, M.A., Dolez, P.I., Dubé, M., David, É., 2017. Development and characterization of a hydrophobic treatment for jute fibres based on zinc oxide nanoparticles and a fatty acid. Appl. Surf. Sci. 397, 19–29.

Ashok, B., Obi Reddy, K., Yorseng, K., Rajini, N., Hariram, N., Siengchin, S., et al, 2018. Modification of natural fibers from Thespesia lampas plant by in situ generation of silver nanoparticles in single-step hydrothermal method. Int. J. Polym. Anal. Charact. 23 (6), 509–516.

Ashok, B., Feng, T.H., Natarajan, H., Anumakonda, V.R., 2019. Preparation and characterization of tamarind nut powder with in situ generated copper nanoparticles using one-step hydrothermal method. Int. J. Polym. Anal. Charact. 24 (6), 548–555.

Ashok, B., Hariram, N., Siengchin, S., Rajulu, A.V., 2020. Modification of tamarind fruit shell powder with in situ generated copper nanoparticles by single step hydrothermal method. J. Bioresourc. Bioproducts 5 (3), 180–185.

Ashok, B., Umamahesh, M., Hariram, N., Siengchin, S., Rajulu, A.V., 2021. Modification of waste leather trimming with in situ generated silver nanoparticles by one step method. Appl. Sci. Eng. Progress 14 (2), 236–246.

ASTM D3039. Standard Test Method for Tensile Properties of Plastics. West Conshohocken, PA: ASTM International; 2014.

Azwa, Z.N., Yousif, B.F., Manalo, A.C., Karunasena, W., 2013. A review on the degradability of polymeric composites based on natural fibers. Mater. Des. 47, 424–442.

Baghaei, B., Skrifvars, M., Salehi, M., Bashir, T., Rissanen, M., Nousiainen, P., 2014. Novel aligned hemp fibre reinforcement for structural biocomposites: Porosity, water absorption, mechanical performances and viscoelastic behaviour. Compos. A Appl. Sci. Manuf. 61, 1–12.

Bak, M., Yimmou, B. M., Csupor, K., Nemeth, R., Csoka, L., 2012. Enhancing the durability of wood against wood destroying fungi using nano-zink. In: International Scientific Conference March, vol. 26, p. 27.

Belaadi, A., Bezazi, A., Bourchak, M., Scarpa, F., Zhu, C., 2014. Thermochemical and statistical mechanical properties of natural sisal fibres. Compos. B Eng. 67, 481–489.

Bessadok, A., Roudesli, S., Marais, S., Follain, N., Lebrun, L., 2009. Alfa fibres for unsaturated polyester composites reinforcement: Effects of chemical treatments on mechanical and permeation properties. Compos. A Appl. Sci. Manuf. 40 (2), 184–195.

Butt, H.J., Cappella, B., Kappl, M., 2005. Force measurements with the atomic force microscope: Technique, interpretation and applications. Surf. Sci. Rep. 59 (1–6), 1–152.

Cosnita, M., Cazan, C., Duta, A., 2017. The influence of inorganic additive on the water stability and mechanical properties of recycled rubber, polyethylene terephthalate, high density polyethylene and wood composites. J. Cleaner Prod. 165, 630–636.

d'Água, R.B., Branquinho, R., Duarte, M.P., Maurício, E., Fernando, A.L., Martins, R., et al, 2018. Efficient coverage of ZnO nanoparticles on cotton fibres for antibacterial finishing using a rapid and low cost in situ synthesis. New J. Chem. 42 (2), 1052–1060.

Dicker, M.P., Duckworth, P.F., Baker, A.B., Francois, G., Hazzard, M.K., Weaver, P.M., 2014. Green composites: A review of material attributes and complementary applications. Compos. Part A: Appl. Sci. Manufa. 56, 280–289.

Ding, W.D., Koubaa, A., Chaala, A., 2012. Dimensional stability of methyl methacrylate hardened hybrid poplar wood. BioResources 7 (1), 0504–0520.

Dittenber, D.B., GangaRao, H.V., 2012. Critical review of recent publications on use of natural composites in infrastructure. Compos. A Appl. Sci. Manuf. 43 (8), 1419–1429.

Donath, S., Militz, H., Mai, C., 2004. Wood modification with alkoxysilanes. Wood Sci. Technol. 38 (7), 555–566.

Farahani, G.N., Ahmad, I., Mosadeghzad, Z., 2012. Effect of fiber content, fiber length and alkali treatment on properties of kenaf fiber/UPR composites based on recycled PET wastes. Polym.-Plastics Technol. Eng. 51 (6), 634–639.

Freeman, M.H., McIntyre, C.R., 2008. Copper-based wood preservatives. Forest Prod. J. 58 (11), 6–27.

Fu, S.Y., Feng, X.Q., Lauke, B., Mai, Y.W., 2008. Effects of particle size, particle/matrix interface adhesion and particle loading on mechanical properties of particulate–polymer composites. Compos. B Eng. 39 (6), 933–961.

Gao, L., McCarthy, T.J., 2008. Teflon is Hydrophilic. Comments on Definitions of Hydrophobicity, Shear versus Tensile Hydrophobicity and Wettability Characterization. Langmuir 24, 9183–9188.

Hadjadj, A., Jbara, O., Tara, A., Gilliot, M., Malek, F., Maafi, E.M., et al, 2016. Effects of cellulose fiber content on physical properties of polyurethane-based composites. Compos. Struct. 135, 217–223.

Hadjadj, A., Jbara, O., Tara, A., Gilliot, M., Malek, F., Maafi, E.M., et al, 2016. Effects of cellulose fiber content on physical properties of polyurethane based composites. Compos. Struct. 135, 217–223.

Hill, C.A., 2007. In: Wood Modification: Chemical, Thermal and Other Processes, Vol. 5. John Wiley & Sons.
JA, M.H., Majid, M.A., Afendi, M., Marzuki, H.F.A., Fahmi, I., Gibson, A.G., 2016. Mechanical properties of Napier grass fibre/polyester composites. Compos. Struct. 136, 1–10.
John, M.J., Anandjiwala, R.D., 2008. Recent developments in chemical modification and characterization of natural fiber-reinforced composites. Polym. Compos. 29 (2), 187–207.
Jotiram, G.A., Palai, B.K., Bhattacharya, S., Aravinth, S., Gnanakumar, G., Subbiah, R., et al, 2022. Investigating mechanical strength of a natural fibre polymer composite using SiO2 nano-filler. Mater. Today:. Proc. 56 (3), 1522–1526.
Jumaidin, R., Sapuan, S.M., Jawaid, M., Ishak, M.R., Sahari, J., 2016. Characteristics of thermoplastic sugar palm Starch/Agar blend: Thermal, tensile, and physical properties. Int. J. Biol. Macromol. 89, 575–581.
Karthikeyan, S., Rajini, N., Jawaid, M., Winowlin Jappes, J.T., Thariq, M.T.H., Siengchin, S., et al, 2017. A review on tribological properties of natural fiber based sustainable hybrid composite. Proc. Inst. Mech. Eng., Part J: J. Eng. Tribol. 231 (12), 1616–1634.
Kulyk, B., Kapustianyk, V., Tsybulskyy, V., Krupka, O., Sahraoui, B., 2010. Optical properties of ZnO/PMMA nanocomposite films. J. Alloy. Compd. 502 (1), 24–27.
Kumar, T., Chandrasekar, M., Senthilkumar, K., Ilyas, R.A., Sapuan, S.M., Hariram, N., et al, 2021. Characterization, thermal and antimicrobial properties of hybrid cellulose nanocomposite films with in-situ generated copper nanoparticles in Tamarindus indica Nut Powder. J. Polym. Environ. 29 (4), 1134–1142.
Kumar, K.P., Sekaran, A.S.J., 2014. Some natural fibers used in polymer composites and their extraction processes: A review. J. Reinf. Plast. Compos. 33 (20), 1879–1892.
Lai, S.M., Kao, Y.H., Liu, Y.K., Chiu, F.C., 2016. Preparation and properties of luffa fiber-and kenaf fiber-filled poly (butylene succinate-co-lactate)/starch blend-based biocomposites. Polym. Test. 50, 191–199.
Li, Y.F., Liu, Y.X., Wang, X.M., Wu, Q.L., Yu, H.P., Li, J., 2011. Wood- polymer composites prepared by the in-situ polymerization of monomers within wood. J. Appl. Polym. Sci. 119 (6), 3207–3216.
Li, X., Tabil, L.G., Panigrahi, S., 2007. Chemical treatments of natural fiber for use in natural fiber-reinforced composites: a review. J. Polym. Environ. 15 (1), 25–33.
Li, Z., Wang, Y., Cheng, L., Guo, W., Wu, G., 2017. Effect of Nano-$CaCO_3$ on the structure and properties of holocellulose-fiber/polypropylene biomass composites. J. Wood Chem. Technol. 37 (1), 62–74.
Li, J., Zhang, J., Natarajan, H., Zhang, J., Ashok, B., Rajulu Anumakonda, V., 2019. Modification of agricultural waste tamarind fruit shell powder by in situ generation of silver nanoparticles for antibacterial filler applications. Int. J. Polym. Anal. Charact. 24 (5), 421–427.
Liang, K., Shi, S.Q., Wang, G., 2014. Effect of impregnated inorganic nanoparticles on the properties of the kenaf bast fibers. Fibers 2 (3), 242–254.
Mohammed, M., Rozyanty, A.R., Osman, A.F., Adam, T., Hashim, U., Mohammed, A.M., et al, 2017. The Weathering Effect in Natural Environment on Kenaf Bast Filled Unsaturated Polyester Composite and Integration of Nano Zinc particle for Water Repellent. Micro Nanosyst. 9 (1), 16–27.
Mohammed, M., Rahman, R., Mohammed, A.M., Osman, A.F., Adam, T., Dahham, O.S., et al, 2018. Effect of kenaf fibre Mat layers and Zinc Oxide Nanoparticle Concentration on the Mechanical and Thermal Properties of ZnONPs/kenaf/polyester Composites. Mater. Sci. Eng. (012079)
Mohammed, M., Rozyanty, R., Mohammed, A.M., Osman, A.F., Adam, T., Dahham, O.S., et al, 2018. Fabrication and characterization of zinc oxide nanoparticle-treated kenaf polymer composites for weather resistance based on a solar UV radiation. BioResources 13 (3), 6480–6496.
Mohammed, M., Betar, B.O., Rahman, R., Mohammed, A.M., Osman, A.F., Jaafar, M., et al, 2019. Zinc Oxide Nano Particles Integrated Kenaf/Unsaturated Polyester Biocomposites. J. Renewable Mater. 7 (10), 967–982.
Mohanty, A.K., Misra, M., Drzal, L.T., Selke, S.E., Harte, B.R., Hinrichsen, G., 2005. Natural fibers, biopolymers, and biocomposites: an introduction, 17–51.
Nosbi, N., Akil, H.M., Ishak, Z.A.M., Bakar, A.A., 2011. Behaviour of kenaf fibers after immersion in several water conditions. BioResources 6 (2), 950–960.
Pandey, J.K., Lee, S., Kim, H.J., Takagi, H., Lee, C.S., Ahn, S.H., 2012. Preparation and properties of cellulose-based nano composites of clay and polypropylene. J. Appl. Polym. Sci. 125 (S1), E651–E660.
Pandey, K.K., Pitman, A.J., 2003. FTIR studies of the changes in wood chemistry following decay by brown-rot and white-rot fungi. Int. Biodeterior. Biodegrad. 52 (3), 151–160.
Papadopoulos, A.N., Mantanis, G.I., 2011. Surface treatment technologies applied to wood surfaces. FDM Asia-Solid Wood Panel Technol. 5, 36–39.
Prasad, V., Joseph, M.A., Sekar, K., Ali, M., 2018. Development of flax fibre reinforced epoxy composite with nano TiO2 addition into matrix to enhance mechanical properties. Mater. Today:. Proc. 5 (5), 11569–11575.
Pukánszky, B., Fekete, E., 1999. Adhesion and surface modification. Mineral Fillers Thermoplast. I, 109–153.
Ray, D., Sarkar, B.K., Rana, A.K., Bose, N.R., 2001. Effect of alkali treated jute fibres on composite properties. Bull. Mater. Sci. 24 (2), 129–135.
Rozman, H.D., Musa, L., Abubakar, A., 2005. Rice husk–polyester composites: the effect of chemical modification of rice husk on the mechanical and dimensional stability properties. J. Appl. Polym. Sci. 97 (3), 1237–1247.
Saiteja, J., Jayakumar, V., Bharathiraja, G., 2020. Evaluation of mechanical properties of jute fibre/carbon nano tube filler reinforced hybrid polymer composite. Mater. Today:. Proc. 22, 756–758.
Salehi, R., Arami, M., Mahmoodi, N.M., Bahrami, H., Khorramfar, S., 2010. Novel biocompatible composite (chitosan–zinc oxide nanoparticle): preparation, characterization and dye adsorption properties. Colloids Surf., B 80 (1), 86–93.
Salem, I.A.S., Rozyanty, A.R., Betar, B.O., Adam, T., Mohammed, M., Mohammed, A.M., 2017. Study of the effect of surface treatment of kenaf fiber on chemical structure and water absorption of kenaf filled unsaturated polyester composite. J. Phys. 012001.
Salman, S.D., Leman, Z., Sultan, M.T.H., Ishak, M.R., Cardona, F., 2016. Influence of fiber content on mechanical and morphological properties of woven kenaf reinforced PVB film produced using a hot press technique. Int. J. Polym. Sci. 2016.
Sanjay, M.R., Madhu, P., Jawaid, M., Senthamaraikannan, P., Senthil, S., Pradeep, S., 2018. Characterization and properties of natural fiber polymer composites: A comprehensive review. J. Cleaner Prod. 172, 566–581.
Sezgin, H., Berkalp, O.B., 2017. The effect of hybridization on significant characteristics of jute/glass and jute/carbon-reinforced composites. J. Ind. Text. 47 (3), 283–296.
Shokrieh, M.M., Kefayati, A.R., Chitsazzadeh, M., 2012. Fabrication and mechanical properties of clay/epoxy nanocomposite and its polymer concrete. Mater. Des. 40, 443–452.
Soltani, M., Najafi, A., Yousefian, S., Naji, H.R., Bakar, E.S., 2013. Water repellent effect and dimension stability of beech wood impregnated with nano-zinc oxide. BioResources 8 (4), 6280–6287.
Sreekala, M.S., Thomas, S., 2003. Effect of fibre surface modification on water-sorption characteristics of oil palm fibres. Compos. Sci. Technol. 63 (6), 861–869.
Sui, X., Liu, Y., Shao, C., Liu, Y., Xu, C., 2006. Structural and photoluminescent properties of ZnO hexagonal nanoprisms syn-

thesized by microemulsion with polyvinyl pyrrolidone served as surfactant and passivant. Chem. Phys. Lett. 424 (4–6), 340–344.
Sun, J.X., Sun, X.F., Zhao, H., Sun, R.C., 2004. Isolation and characterization of cellulose from sugarcane bagasse. Polym. Degrad. Stab. 84 (2), 331–339.
Thooyavan, Y., Kumaraswamidhas, L.A., Raj, R.E., Binoj, J.S., 2022. Influence of SiC micro and nano particles on tribological, water absorption and mechanical properties of basalt bidirectional mat/vinyl ester composites. Compos. Sci. Technol. 219, 109210.
Traistaru, A.T., Timar, M.C., Campean, M., Croitoru, C., Sandu, I.O. N., 2012. Paraloid B72 versus Paraloid B72 with nano-ZnO additive as consolidants for wooden artefacts. Mater. Plast 49, 293–300.
Tshabalala, M.A., Libert, R., Schaller, C.M., 2011. Photostability and moisture uptake properties of wood veneers coated with a combination of thin sol-gel films and light stabilizers. Holzforschung 65 (2), 215–220.
Valadez-Gonzalez, A., Cervantes-Uc, J.M., Olayo, R.J.I.P., Herrera-Franco, P.J., 1999. Effect of fiber surface treatment on the fiber–matrix bond strength of natural fiber reinforced composites. Compos. B Eng. 30 (3), 309–320.
Wambua, P., Ivens, J., Verpoest, I., 2003. Natural fibers: can they replace glass in fibre reinforced plastics? Compos. Sci. Technol. 63, 1259–1264.
Wang, X., Liu, J., Chai, Y., 2012. Thermal, mechanical, and moisture absorption properties of wood-TiO2 composites prepared by a sol-gel process. BioResources 7 (1), 0893–0901.
Wang, H., Lu, R., Huang, T., Ma, Y., Cong, P., Li, T., 2011. Effect of grafted polytetrafluoroethylene nanoparticles on the mechanical and tribological performances of phenol resin. Mater. Sci. Eng., A 528 (22–23), 6878–6886.
Wegner, T.H., Winandy, J.E., Ritter, M.A., 2005. Nanotechnology opportunities in residential and non-residential construction. 2nd International Symposium on Nanotechnology In Construction.
Wong, K.J., Yousif, B.F., Low, K.O., 2010. The effects of alkali treatment on the interfacial adhesion of bamboo fibres. Proc. Inst. Mech. Eng., Part L: J. Mater.: Design Appl. 224 (3), 139–148.
Xiong, M., You, B., Zhou, S., Wu, L., 2004. Study on acrylic resin/titania organic–inorganic hybrid materials prepared by the sol–gel process. Polymer 45 (9), 2967–2976.